Chemical Science

REVIEW



Cite this: Chem. Sci., 2022, 13, 3082

Received 9th November 2021 Accepted 15th February 2022

DOI: 10.1039/d1sc06231j

1. Introduction

Bulk hydrogels are polymeric networks that are filled with a large quantity of water. The ability to render them biocompatible and the large quantity of water contained in them makes them attractive for many biomedical applications including for wound healing,¹ as drug carriers,² and in tissue engineering to support cell culture^{3,4} or cartilage replacements.⁵ Hydrogels are most frequently manufactured from bulk solutions containing molecular building blocks. These building blocks are converted into a percolating network either by polymerizing monomer units or by crosslinking appropriate oligomers or polymers. The resulting bulk hydrogels typically possess a homogeneous composition and an ill-defined microstructure, limiting possibilities to control the mechanical properties and introduce spatially confined functionalities to the hydrogels. These shortcomings can be addressed if hydrogels are made of hydrogel-based microparticles, so-called microgels, that are densely packed. Microgels are most commonly fabricated from emulsion drops that are filled with appropriate reagents, or from the fragmentation of crosslinked bulk hydrogels, as was extensively discussed in previous work.6,7 The obtained microgels are then jammed into a paste-like granular hydrogel precursor. The use of microgels as building block of macroscopic hydrogels bears the distinct advantage that it enables abrupt, non-linear compositional changes if granular hydrogels are made of multiple types of microgels possessing distinctly

Mechanical reinforcement of granular hydrogels

Alvaro Charlet, D Francesca Bono and Esther Amstad \textcircled{D}^{*}

Granular hydrogels are composed of hydrogel-based microparticles, so-called microgels, that are densely packed to form an ink that can be 3D printed, injected or cast into macroscopic structures. They are frequently used as tissue engineering scaffolds because microgels can be made biocompatible and the porosity of the granular hydrogels enables a fast exchange of reagents, waste products, and if properly designed even the infiltration of cells. Most of these granular hydrogels can be shaped into appropriate macroscopic structures, yet, these structures are mechanically rather weak. The poor mechanical properties prevent the use of these structures as load-bearing materials and hence, limit their field of applications. The mechanical properties of granular hydrogels depend on the composition of microgels and the interparticle interactions. In this review, we discuss different strategies to assemble microparticles into granular hydrogels and highlight the influence of inter-particle connections on the stiffness and toughness of the resulting materials. Mechanically strong and tough granular hydrogels have the potential to open up new fields of their use and thereby to contribute to fast advances in these fields. In particular, we envisage them to be well-suited as soft actuators and robots, tissue replacements, and adaptive sensors.

different compositions.⁸ This possibility has been exploited to guide cell proliferation.⁹ To strengthen inter-particle interactions, and thereby increase the stiffness of the granular hydrogels under tension, adjacent microgels are often connected either through their surfaces or a second percolating network, resulting in annealed particle scaffolds, or granular hydrogels; here, we refer to the formation of inter-particle connections as curing.

The use of deformable particles to assemble a macroscopic material offers an additional advantage: it enables control over the microstructure by tuning the size, size distribution, and packing density of the microgels. Moreover, this procedure strongly facilitates the fabrication of macroscopic materials possessing well-defined 3D shapes through dip-coating¹⁰ and injection^{9,11-13} because it decouples the rheological properties of the precursor solution from those of the ink. This asset even enables 3D printing of structures possessing intricate shapes that cannot be fabricated with casting methods using commercially available extrusion-based bioprinters.¹⁴

1.1 Applications of granular hydrogels

Granular hydrogels display properties that are distinctly different from those of bulk hydrogels. For example, they possess rheological properties that are ideal for bioprinting^{15,16} and tissue repair.¹⁷ Moreover, they inherently possess a percolating porosity, such that they fulfill many of the numerous requirements advanced tissue engineering applications impose on materials, as was nicely summarized in previous work.^{6,7} In particular, tissue engineering applications often require the



View Article Online

View Journal | View Issue

Soft Materials Laboratory, Institute of Materials, EPFL Lausanne, Lausanne 1015, Switzerland. E-mail: esther.amstad@epfl.ch

View Article Online Chemical Science

precursors to possess multiple functionalities, be biocompatible, degradable,18 and injectable.11 Moreover, their processing into superstructures must be biocompatible.16 The resulting superstructures must enable cells to proliferate through percolating pores such that they can populate the entire scaffold over time,19 and possess locally tunable chemistries, including biochemical and mechanical gradients,5,20,21 to direct cell differentiation and growth. In addition, they should have specific viscoelastic properties that drive proper cell fate and activity. These time-dependent mechanical properties, in particular stress relaxation and creep, impact cell behaviors such as cell spreading, proliferation, and differentiation²²⁻²⁴ and are thus imperative to control if scaffolds are used for tissue engineering. Hydrogels used for tissue engineering are typically soft and degradable such that cells can remodel them or grow their own extracellular matrix (ECM) within them. These features are especially important if hydrogels are used as scaffolds for the growth of functional organoids,25 neural interfaces²⁶ or cartilage.²⁷ The viability and fate of cells can be further tuned through the addition of appropriate chemical receptors, growth factors, and nutrients.18 Granular hydrogels are particularly attractive to tune these features because of their inherent porosity and the short diffusion lengths within the microgels that enable their efficient functionalization. For example, different chemicals can be infiltrated into microgels to control the local composition of granular hydrogels on a micrometer length scale.

The requirements imposed on hydrogels used as tissue replacements are fundamentally different: these hydrogels should be tough and strong¹⁴ yet resilient²⁸ to match the tissue mechanics of targeted natural tissues such as tendons^{29,30} or cartilage.³¹ Typically, tough and strong hydrogels are achieved by a double network architecture.^{32,33} Feasibility to design tough and strong hydrogels that are also resilient has been demonstrated by increasing the entanglement density within the networks.³⁴ However, the potential of these hydrogels in applications remains to be shown.

To meet the demanding and versatile requirements that advanced biomedical and material science applications impart on hydrogels, their structure and composition must be closely controlled and often locally varied. These needs demand for new materials that possess well-defined, locally changing compositions and controllable structures on the nanometer up to the millimeter lengths scales. Granular hydrogels have the potential to meet these requirements as they can be made from microgels possessing well-defined sizes and distinctly different compositions. In this review, we will explore the relationship between the inter-microgel interactions, and the rheological and mechanical properties of the corresponding granular hydrogels. We will introduce the characteristics and design principles of microgel based materials and discuss different strategies to reinforce granular constructs by connecting microgels. Within this framework, we will highlight emerging possibilities to design mechanically robust materials by taking advantage of the recently obtained insights into the influence of the composition and inter-particle connections on the mechanical properties of granular materials.

2. Characteristics of microgel based materials

2.1 Microgel fabrication

Granular hydrogels are produced in two steps: a precursor solution is initially processed into individually dispersed microgels that are assembled into superstructures in a second step, as was nicely summarized in recent reviews.^{6,7} Microgels are commonly fabricated through a bottom-up method from emulsion drops that are filled with appropriate reagents. These drops are formed through batch emulsification,¹⁴ electrohydrodynamic spraying,³⁵ or microfluidics³⁶ and converted into microgels by solidifying the reagents contained in them. The resulting microgels are spherical and possess diameters between a few µm and a few 100 µm. Alternatively, microgels are fabricated through lithography,^{37,38} or using a top-down approach: mechanical fragmentation.³⁹ These microgels are non-spherical and have diameters between a few 100 µm.

Microgels are typically fabricated from biopolymers, monomers, or oligomers.6 Commonly used biopolymers include alginate,⁴⁰ gelatin,⁴¹ chitosan,⁴² and hyaluronic acid^{9,43} with molecular weights superior to 20 kDa; these biopolymers are often functionalized with multiple reactive groups that are covalently connected to their chains. Monomers are most commonly based on acrylates or methacrylates that can be solidified through radical polymerization reactions. The most frequently reported oligomer is end-functionalized poly(ethylene glycol) (PEG), often composed of multi-armed telechelic chains with a molecular weight between 3 and 20 kDa. The intra-particle mechanical properties are determined by the degree of crosslinking of the reagents the particles are made from and can be tuned over a wide range.44 The resulting microgels are typically washed to remove residues of oil and surfactants before they are swollen to equilibrium in an aqueous solution.6 They are subsequently jammed using centrifugation or vacuum filtration to form a shear thinning ink that can be further processed into macroscopic materials.7

2.2 Jammed microgels as inks

Jammed microgels form a soft viscoelastic material that displays peculiar rheological properties, which are similar to other jammed media such as jammed colloidal poly(methylmethacrylate), silica or LAPONITE[®].^{45,46} Unlike microgels that are dispersed in water, jammed microgels are physically constrained by their neighbors limiting their mobility. In the jammed state, individual microgels are held together by weak interparticle forces that impart elasticity to the media. The weak adhesive forces between soft microgels are associated with interstitial liquid bridges that form between adjacent microgels or frictional forces.47,48 Jammed microgels collectively behave as a Bingham plastic⁴⁹ - they are shear thinning, have a low yield stress, and promptly recover their solid-like behavior after high shear stresses are released. These properties are closely correlated to the packing degree, which is higher for soft deformable particles than for hard counterparts.50

Chemical Science

Jammed microgels are ideal for injection, extrusion, casting and 3D printing applications.^{6,7} The shear thinning behavior and low yield stress enable extrusion through a nozzle under ambient conditions with low pressures (1–100 kPa).⁴³ The fast recovery of the solid properties enables extrusion of shaperetaining stable filaments, as sketched in Fig. 1a, and contributes to the good shape fidelity of 3D printed granular objects.

3. Reinforcement techniques of granular hydrogels

Jammed microgels typically interact through non-specific physical inter-particle forces, such that they display a low yield stress and easily deform when subjected to mechanical strain. These properties are desirable if used for tissue engineering applications. However, they prevent the use of these materials for load-bearing applications. The mechanical properties of granular hydrogels can be improved by strengthening inter-particle interactions, for example by crosslinking adjacent particles through strong physical or chemical links, herein referred as curing. This curing step imparts elasticity to the granular hydrogels beyond the yield stress of the original jammed microgels, as sketched in Fig. 1a. More generally, the mechanical properties of granular hydrogels can be tuned with the inter-particle crosslinking strategy, as exemplified in Fig. 1b and c. Indeed, by exploiting the vast range of bond types in organic polymeric networks, the viscoelastic properties of granular hydrogels can be tuned over a considerable range. In this review, we will classify the strategies used to connect adjacent microgels into binding mechanism groups, namely covalent interactions, the use of binders and additives, coordination interactions, electrostatic interactions, other supramolecular interactions, and interpenetrating networks, as summarized in Fig. 2d-i and demonstrated in Fig. 3. We will discuss the impact of the inter-particle binding strategy on the elastic properties of granular hydrogels, such as the oscillatory storage modulus, the compressive modulus, and the tensile Young's modulus. We conclude the review by demonstrating that granular hydrogels cured with a well-designed interparticle binding strategy open up completely new fields of their use that include the manufacturing of load-bearing recyclable materials.

3.1 Covalent interactions

3.1.1 Radical polymerization of methacrylates. Microgels can be synthesized to present chemically active sites at their surfaces such that they can form covalent inter-particle bonds. A common chain-growth mechanism used to form microgels and to covalently link them is the free-radical polymerization of acrylates and methacrylates. This solidification and connection

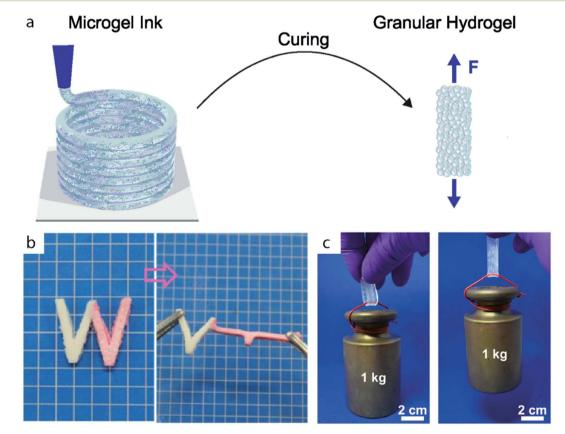


Fig. 1 (a) Microgels are assembled and cured to form granular hydrogels. (b) W-shaped stripe of granular hydrogel composed of microgels with two different Young's moduli. The microgels are cured through electrostatic interactions. Adapted with permission.⁵¹ (c) Stripe of double network granular hydrogel holding a 1 kg weight. Adapted with permission.¹⁴

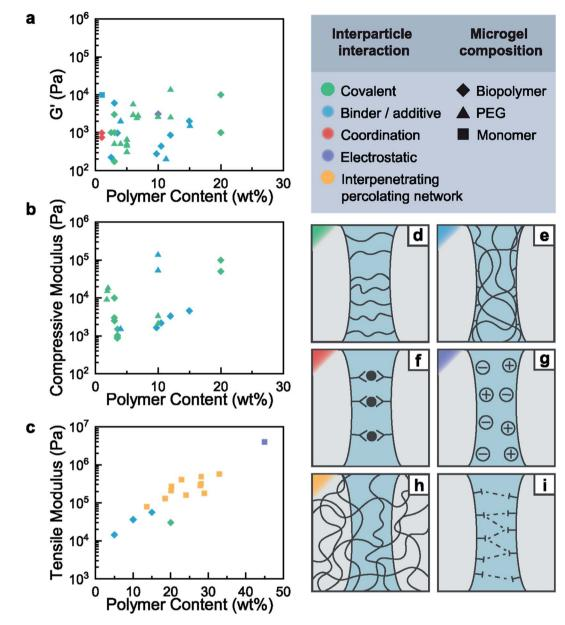


Fig. 2 Elastic mechanical properties of granular hydrogels cured through various interparticle binding strategies. Ashby plots of the storage (a), compressive (b), and tensile (c) modulus as a function of polymer content. Schematic representation of the interparticle interaction mechanisms: covalent interaction (d), binder and additives (e), coordination interactions (f), charge interactions (g), interpenetrating percolating network (h) and other supramolecular interactions (i).

strategy is attractive because of the large range of commercially available monomers, their ease of use, and the good mechanical properties of the resulting polymerized materials. Methacrylates are particularly suited for biomedical applications because they are compatible with many biological systems³⁷ and react under ambient wet conditions.⁵³

Covalent crosslinking of microgels composed of physically crosslinked networks requires a chemical modification of the polymers prior to their conversion into microgels. This is commonly done for naturally occurring biopolymers, such as gelatin or alginate that are functionalized with acrylates or methacrylates.^{41,52,54} For example, microgels composed of thermally gelled gelatin, or ionically crosslinked alginate, expose dangling methacrylate groups. A simple UV-triggered polymerization enables the formation of strong permanent bonds between adjacent microgels. The resulting granular hydrogels possess storage moduli ranging from a few kPa^{41,54,55} to 10 kPa.⁵⁶ Within 60 s of moderate UV exposure (10 mW cm⁻²), jammed microgels are converted into granular hydrogels with a compressive modulus of 100 kPa and a tensile modulus of 30 kPa;⁵⁶ these mechanical properties are similar to those of a human muscle. However, radical polymerization is prone to oxygen quenching, which can compromise the crosslinking efficiency and lead to inferior mechanical properties of granular

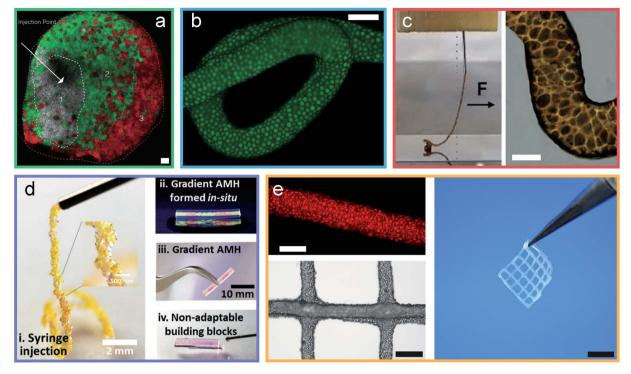


Fig. 3 Granular hydrogels are cured through different inter-particle interactions. (a) Micrograph of an injected, and covalently cured granular hydrogel.⁹ (b) Micrograph of an extruded filament of jammed microgels cured into a granular hydrogel using a binder.⁴³ (c) Image and micrograph of a granular hydrogel cured using coordination chemistry.¹³ (d) Images of a granular hydrogel cured by charged interactions.⁵² (e) Micrographs and image of a double network granular hydrogel.¹⁴ Scale bars are (a) 100 μm, (b) 500 μm, (c) 100 μm, (d) 2 mm and 10 mm, (e) 500 μm, 1 mm and 5 mm. Adapted with permission.

hydrogels.⁵³ Furthermore, despite the increased biocompatibility of methacrylate radical reactions compared to those of acrylates, free-radical reactions are incompatible with certain biologically active tissues. Residual free radicals can induce oxidative stress on human tissues, which is associated to serious chronic diseases such as cancer and osteoporosis.⁵⁷

3.1.2 Click chemistry reactions. Click chemistry reactions occur between two well-defined chemical moieties that covalently bind to each other when they approach each other. These reactions overcome some of the limitations of free-radical acrylate-based reactions because they are efficient, selective, less sensitive to the presence of oxygen, have high yields and can be performed under ambient conditions without producing biologically harmful byproducts.58,59 In particular, two types of thiol-ene reactions have gained attraction. The first is a photomediated radical crosslinking method between molecules containing thiols and those containing -enes. This method is particularly widely used by the biomaterial community owing to the vast range of available starting materials.⁶⁰ The second heavily used reaction, is a base-catalyzed Michael-type conjugate addition of thiols to electron deficient alkenes such as acrylates, vinyl sulfones and maleimides.61-63 This reaction can be performed under mild conditions in the absence of freeradicals, which makes it ideal for *in situ* gelation of hydrogels intended for in vivo applications.64,65 While both these crosslinking strategies have been used to synthesize microgels,^{2,11,43,43,44,55,66-77} they are much more rarely used to cure

granular hydrogels. This shortcoming is most probably related to the limited availability and mobility of reactive groups at the surfaces of microgels. An azide alkyne click reaction has been reported to cure granular hydrogels by mixing two populations of microgels, one containing excess azides, and the other excess alkyne groups. The resulting granular hydrogels displayed compressive moduli of 2-3 kPa.78 This approach requires a very high control over stoichiometric ratios of the reagents, and is synthetically more involved than radical polymerization reactions, due to the limited commercial availability of reactants. Furthermore, microgels composed of end-functionalized crosslinked polymers tend to have limited numbers of reactive groups on their surfaces. The limited number of reactive groups available at the microgel surface inhibits the formation of a sufficient number of load-transferring inter-particle bonds. As a result, granular hydrogels that were cured through this approach typically display poor mechanical properties, they are much weaker than the constituting microgels.78

3.1.3 Enzymatic coupling reactions. Enzymes drive reactions with product selectivity and yields beyond what is achieved by engineered catalysts. One of the most prominent examples of enzymatically driven mechano-morphing events is the formation of blood clots during hemostasis.^{79,80} This fast sol-gel transition is triggered by the covalent crosslinking of the supramolecular assembly of fibrin chains into macroscopic fibers. The covalent crosslinking occurs between amine groups present in glutamines and lysine peptides and is initiated by

Review

enzyme XIIIa. This fast and selective process inspired the use of enzyme XIIIa as the curing agent of synthetic granular hydrogels.^{2,9,66,68,70,71,74,75,77} These granular hydrogels were composed of microgels with dangling lysine- and glutamine-containing peptides; these sites were used to cure the granular hydrogels after the microgels have been shaped into the desired macroscopic granular materials. The resulting materials have a compressive modulus of 1-20 kPa and a storage modulus of 0.5-15 kPa, which are in the order of soft biological tissues such as the skin or muscles. Their softness can be attributed to the low density of binding sites at the microgel interfaces that results in a low inter-particle crosslink density and hampers the use of such granular hydrogels for load-bearing applications. Enzymes have also been used to increase the stiffness and toughness of bulk hydrogels by inducing the mineralization of amorphous calcium phosphate.81 Taking advantage of these insights, the vast range of available enzymatically driven reactions could be harnessed to crosslink microgels. However, to take full advantage of this strategy, the microgel formation and curing mechanism would have to be tailored to ensure a high density of reactive groups present at the microgel surface and that their mobility is sufficiently high. These assets would enable the formation of a high density of inter-particle links that ensures an efficient load transfer between adjacent microgels, which would translate into an increased stiffness of the granular hydrogels.

3.2 Binder and additives

A recurrent limitation of the previously described cases is the low mobility of reactive groups on the microgel's surface, that prevents an efficient formation of inter-particle connections. This limitation can be overcome if adjacent particles are connected through binders because they are typically dissolved in a liquid surrounding the microgels, such that they possess a high mobility. This feature has been demonstrated on microgels that were synthesized using a click chemistry reaction, norbornene-thiol. The molar ratio of the reagents contained within the drop template was not stoichiometric such that some norbornene groups remained active even after the microgels have been formed. These reactive sites could be used to form inter-particle connections by exposing them to a solution containing linear polyethylene glycol (PEG) that was endfunctionalized with thiol groups.44 Another study reports the use of a curing solution containing a short di-thiol molecule and norbornene-functionalized hyaluronic acid, which efficiently cured microgels presenting the same reactive groups at their surfaces to covalently crosslink them at a high density. The high crosslinking density can be assigned to the deformation of soft microgels that increases the contact area between adjacent microgels and hence, the density of inter-particle crosslinks, when the bridging molecule is of low molecular weight. As a result, these granular hydrogels displayed a compressive modulus of 5 kPa.43 This result hints at the importance of the inter-particle contact area and the associated inter-particle crosslink density for the mechanical properties of granular materials.

Binders can be composed of low molecular weight polymers that possess a high mobility. Even if the di-functional binders with a molecular weight as low as 3400 Da are used to connect adjacent microgels, the storage moduli of the resulting granular hydrogels can reach values between 0.2 to 1.5 kPa.44,76 This result demonstrates that even low molecular weight crosslinkers can efficiently form covalent bonds between adjacent microgels. We again attribute this feature to the softness of the microgels that allows them to deform, thereby maximizing the contact area between adjacent microgels. Alternatively, microgels can be connected through higher molecular weight binders that possess multiple functionalities, such as 4-armed PEG (20 kDa). The resulting granular hydrogels display storage moduli between 0.2 to 2 kDa and compressive moduli in the range of 1-5 kPa.^{69,72,73,82} The storage modulus can be increased up to 6 kPa if higher molecular weight multi-functionalized biopolymers are used, such as hyaluronic acid (HA).¹¹ This result indicates that the inter-particle crosslinking efficiency increases with increasing molecular weight of the crosslinker, most likely because of the higher flexibility of these molecules. A general limitation of this approach is the poor control over the exact concentration of binding polymers at the microgel interfaces. This parameter is directly related to the packing degree of jammed microgels, and the affinity of binders to the microgel surface and is hence difficult to systematically vary. As a result of this limitation, the mechanical properties of the resulting granular hydrogels cannot be deliberately tuned over a wide range.

Microgels can also be dispersed in a matrix without being covalently linked to it. For example, a gelatin matrix has been reinforced with microgels composed of gelatin with a higher concentration than the matrix. The Young's modulus of the composite under tension is 40 kPa, 8-times that of the matrix alone. This microgel-induced stiffening is attributed to the physical interactions between gelatin chains.⁸³ However, the control over the microstructure of the resulting composites is limited because the microgels are not jammed and randomly distributed within the matrix material.

3.3 Supramolecular interactions

3.3.1 Physical and coordination bonds. Previously discussed granular hydrogels are mostly composed of microgels that are irreversibly connected to each other through covalent bonds. Irreversible inter-particle connections typically result in rather brittle granular hydrogel, because microgels cannot rearrange if subjected to stress, and the mechanisms that dissipate energy and thereby prevent a catastrophic failure are limited. This shortcoming can be overcome if microgels are reversibly crosslinked through supramolecular interactions. For example, microgels composed of carboxylated cellulose have been cured by exposing them to a Ca²⁺-containing solution. The resulting granular hydrogels whose microgels are physically connected to each other possess storage moduli between 0.5 to 1 kPa, similar to those of microgels that have been connected through covalent binders.84 Stronger inter-particle bonds can be formed if metal-ligand coordination chemistry is used, whose

Chemical Science

binding strength is close to the one of covalent bonds.85 Extensive research has been done on harnessing coordination chemistries to design dynamic, viscoelastic, self-healing bulk hydrogels whose mechanical properties can be tuned with the choice of the type of chelator and metal ion.⁸⁶ A similar strategy has been employed to link adjacent microgels that have been functionalized with pyrogallols. Pyrogallols possess a high affinity to certain metal ions, such as Fe³⁺.⁸⁷ Moreover, they can catalyze the reduction of certain ions, such as Ag⁺, resulting in the formation of silver nanoparticles. The latter strategy has been used to fabricate granular hydrogels whose grain boundaries were reinforced with silver nanoparticles. However, the mechanical properties of the resulting granular hydrogel were poor, with a storage modulus reaching only 0.13 kPa.13 The poor contribution of the pyrogallol nanoparticle complexes to the elasticity of the granular hydrogels suggests that the pyrogallols have limited mobility and cannot significantly contribute to interparticle bonding. Hence, while metal-ligand coordination chemistries have been successfully used to design advanced bulk hydrogels, their use as efficient inter-particle crosslinkers

remains to be shown. 3.3.2 Electrostatic interactions. The marine sandcastle worm uses a variety of supramolecular interactions to form strong granular media. These fascinating mechanical properties are a result of strong adhesive coacervates that link adjacent grains. Inspired by the marine sandcastle worm, hydrogels have been reinforced with oppositely charged polymers. For example, a single percolating polyelectrolyte network was swollen with oppositely charged monomers to form a secondary network. Importantly, the second network was formed in a saline solution to speed up the swelling of the first network that ensures a homogeneous distribution of the second type of monomers also within the microgels.⁵¹ The resulting swollen microgels were subsequently dialyzed to cancel ion screening, resulting in a poly-ion complex between positively and negatively charged strands located within and between microgels. The strong ion interactions between microgels resulted in fracture strengths of the resulting granular hydrogels that are as high as 1.5 MPa, and a Young's modulus of 4 MPa, orders of magnitude superior to the same sample under saline conditions.⁵¹ Interestingly, the use of saline solutions to screen ionic bonding, as a reversible on/off switch of ionic interactions yields promising use for additive manufacturing applications under mild conditions.

Positive and negative charges can also be separated in space by using a mixture of cationic and anionic polyelectrolyte microgels to form granular hydrogels.⁵² This concept was nicely demonstrated on granular hydrogels composed of a mixture of chitosan-based and gelatin-based microgels. At neutral pH, chitosan is a cationic polyelectrolyte, whereas gelatin is an anionic one. The resulting granular hydrogel has a storage modulus of 3 kPa. This value is significantly lower than that of granular hydrogels whose microgels are connected through polyionic complexes, due to a lower coulombic attraction between charged microgel surfaces, and the limited contact areas between adjacent microgels.

3.4 Secondary percolating network

The vast majority of granular hydrogels are cured by linking adjacent microgels through their interfaces. This crosslinking strategy requires a high degree of control over the availability and mobility of chemical groups to ensure an efficient load transfer between microgels, a requirement that is synthetically demanding. An alternative approach is to embed the microgels within a percolating network that transfers load from microgel to microgel over a larger volume, reducing locally high strains that typically lead to catastrophic failure of the material. Using this approach, the curing of the granular hydrogel is not only based on local adhesion between microgels, but on the cohesion of the percolating network. Microgels dispersed in a hydrogel matrix can act as reinforcing fillers⁸⁸ because they contribute sacrificial bonds. Hence, their effect on the mechanical properties of the composite hydrogels is similar to that of the sacrificial network in double network hydrogels. To increase the density of microgels within the hydrogel matrix and thereby the control over the microstructure of the material, dried grinded microgels can be directly soaked in solution containing monomers that are used for the assembly of the secondary network. Upon polymerization of the secondary percolating network, a granular hydrogel with a 250 kPa Young's modulus can be achieved.¹⁰ However, this granular hydrogel has only been reported as a thin hydrogel coating. Much larger granular structures can be produced from emulsion templated microgels that are soaked in a monomercontaining solution. Jamming of the monomer-loaded microgels allows their 3D printing into macroscopic structure. This structure is cured by polymerizing the reactive monomers contained in the microgels. By controlling the ratio between the two polymeric networks, the Young's moduli of the resulting double network granular hydrogels can be tuned from 20 kPa up to 570 kPa,14 a value close to the elasticity of human cartilage and exceeding Young's moduli of any of the previously reported 3D printed hydrogels. The extraordinarily high mechanical properties are attributed to the efficient load transfer from the secondary network by distributing the load transfer onto the primary microgel network in space, beyond the microgel interfaces. This reinforcing strategy offers an additional advantage: through the introduction of reversible covalent crosslinks in the percolating network, double network granular hydrogels can be selectively degraded into dispersed microgels. The washing of the microgels and subsequent swelling with a pristine solution of monomers enables the recycling of the microgels into a novel granular hydrogel that is even stiffer than the pristine once such that this material is well-suited for loadbearing applications even after having been recycled five times. If the recyclable double network granular hydrogel is dried, it has a similar stiffness to that of commercial plastics such as acrylonitrile butadiene styrene (ABS), polyethylene (PE), and polyethylene terephthalate (PET), yet it can be recycled under benign conditions within 2 hours.89 This proof-of-concept strategy emphasizes that granular hydrogels cured with welldesign interparticle interactions have promising applications

This article is licensed under a Creative Commons Attribution-NonCommercial 3.0 Unported Licence. Open Access Article. Published on 15 2022. Downloaded on 15.08.2025 19:24:16. (cc) BY-NC

microgel size, the average polymer content, the storage modulus (G'), the compression modulus (E_{comp}) and the tensile modulus (E_{tens}) are reported as a function of the interaction type and Table 1 List of reported granular hydrogels, composed of either monomers (monom.), oligomers (PEG) or biopolymers (biop.) as a function of their interaction type. The values of the average microgel composition

type Microgel composition Radical polym. Biop. Ox. Alg-MA Gel-MA Gel-MA Gel-MA Click Biop. HAacyl. + di-SH Biop. HAacyl. + di-SH HAacyl. + di-SH Click Biop. HAacyl. + di-SH PEG 4 PEG-axide (10 kDa) + 8 PEG-allyne (20 kDa) Enzym. Biop. HAacyl. + di-SH PEG 4 PEG-38 (20 kDa) + di-SH PEG 4 PEG-38 (20 kDa) + di-SH 4 PEG-38 (20 kDa) + di-SH 4 PEG-38 (10 kDa) 4 PEG-38 (20 kDa) + di-SH 4 PEG-38 (10 kDa) 4 PEG-38 (20 kDa) + di-SH 4 PEG-38 (10 kDa) 4 PEG-38 (20 kDa) + di-SH 4 PEG-38 (10 kDa) 4 PEG-38 (20 kDa) + di-SH 4 PEG-38 (10 kDa) 10 kDa HANB + di-SH. Binder: 4 PEG-36 (10 kDa) 11 ANB + di-SH. Binder: 4 PEG-36 (10 kDa) 10 kDa) + di-SH 12 kDa 20 kDa 10 kDa) + di-SH 13 kDa 20 kDa 10 kDa) + di-SH 14 kDA 20 kDa 13 kDa) 15 kDA 10 kDa 13 kDa) 16 kDA 10 kDA 13 kDA 17 kDA 10 kDB 13 kDA 18 kDA 10 kDB 13 kDA 18 kDA 20 kDB 14 kDA <t< th=""><th>0</th><th><i>C</i></th><th>5</th><th>$E_{\rm c}$</th><th>$E_{\rm t}$</th><th></th></t<>	0	<i>C</i>	5	$E_{\rm c}$	$E_{\rm t}$	
Radical polym. Biop. Ox. Alg-MA Redical polym. Biop. 4-PEG-axide (10 kDa) + 8-PEG-allyne (20 Click Biop. HA-acryl. 4 di:SH Biop. HA-acryl. 4 di:SH PEG 4-PEG-axide (10 kDa) + 8-PEG-allyne (20 Raym. Biop. HA-acryl. 4 di:SH PEG 4-PEG-vs (20 kDa) + di:SH Rec-vs (20 kDa) + di:SH 4-PEG-vs (20 kDa) + di:SH Rec-vs (20 kDa) + di:SH 4-PEG-vs (20 kDa) + di:SH Rec-vs (20 kDa) + di:SH 8-PEG-vs (20 kDa) + di:SH Rec-vs (20 kDa) + di:SH 8-PEG-vs (20 kDa) + di:SH Rec-vs (20 kDa) + di:SH 8-PEG-vs (20 kDa) + di:SH Rec-vs (20 kDa) + di:SH Bioder: 4-PEG-tetrazine Rec-vs (20 kDa) + di:SH Bioder: 2-PEG-SH (3, 4 kDa) Rec-vs (20 kDa) + di:SH Bioder: 4-PEG-tetrazine Rec-vs (20 kDa) + di:SH Bioder: 2-PEG-SH (3, 4 kDa) Rec-vs (20 kDa) + di:SH Bioder: 2-PEG-SH (3, 4 kDa) Rec-vs (20 kDa) + di:SH Bioder: 2-PEG-SH (3, 4 kDa) Rec-vs (20 kDa) + di:SH Bioder: 2-PEG-SH (3, 4 kDa)	(mn)	(wt%)	(kPa)	(kPa)	(kPa)	Ref.
Cel-MA PEG 4-PEG-MA_MA (20 kDa) Enzym. Bjop. HAaeryl. 4i:SH Rog. HAaeryl. 4i:SH Braym. Bjop. HAaeryl. 4i:SH HAaeryl. 4i:SH PEG 4-PEG-vS (20 kDa) + di-SH HAaeryl. 4i:SH PEG 4-PEG-VS (20 kDa) + di-SH 4-PEG-VS (20 kDa) + 2-PEG-SH (3.4 kDa) 2-PEG-NB (5-20 kDa)	300	2.5	-1	I	I	54
Click Biop. HAacryl. 4di-SH Biop. HAacryl. 4di-SH PEG 4-PEG-axide (10 kDa) + 8-PEG-allyne (20 RDa) Enzym. Biop. HAacryl. 4di-SH PEG 4-PEG-VS (20 kDa) + di-SH PEG 4-PEG-VS (20 kDa) + 2-PEG-SH (3.4 kDa) PEG-NHS (20 kDa) + 2-PEG-SH (3.4 kDa) PEG PEG PEG PEG PEG PEG PEG PEG PEG PEG	140	20	1	100	30	41
PEG 4-PEG-MAL-MA (20 kDa) FEG 4-PEG-axide (10 kDa) + 8-PEG-allyne (20 kDa) Enzym. Biop. HA-acryl. + di-SH FEG 4-PEG-vs (20 kDa) + di-SH HA-acryl. + di-SH HA-acryl. + di-SH FEG 4-PEG-vs (20 kDa) + di-SH HA-acryl. + di-SH HA-BEG-VS (20 kDa) + 2-PEG-SH (3.4 kDa) HA-BE di-SH Binder: 4-PEG-tetrazine (20 kDa) HA-NB + di-SH. Binder: 4-PEG-tetrazine (20 kDa) NHS coupling Biop. Gel-NB + 2-PEG-SH (3.4 kDa)	90	20	10	50		56
Click Biop. HAacryl. + di-SH PEG 4-PEG-azide (10 kDa) + 8-PEG-allyne (20 kDa) Enzym. Biop. HAacryl. + di-SH HAacryl. + di-SH PEG 4-PEG-VS (20 kDa) + di-SH RABCH 4-PEG-VS (20 kDa) + di-SH RPEG-VS (20 kDa) + 2-PEG-SH (3 4 kDa) NHS coupling Biop. RA-NB + di-SH. Binder: 4-PEG-tetrazine (20 kDa) RA-NB + di-SH. Binder: 2-PEG-SH (3 4 kDa) NHS coupling Biop. RA-NB + di-SH. Binder: 4-PEG-tetrazine (20 kDa) RA-NB + di-SH. Binder: 2-PEG-SH (3 4 kDa) NHS coupling Biop. Gel-NB (5-20 kDa) + 2-PEG-SH (3 4 kDa) NHS coupling Biop. Gel-NB (5-20 kDa) + 2-PEG-SH (3 4 kDa) NHS coupling Biop. Gel-NB (5-20 kDa) + 2-PEG-SH (3 4 kDa) Ratrix Biop. Gel-NB (5-20 kDa) + 2-PEG-SH (3 4 kDa) NHS coupling Biop. Gel-NB (5-20 kDa) + 2-PEG-SH (3 4 kDa) NHS coupling Biop. Gel-NB (5-20 kDa) + 2-PEG-SH (3 4 kDa) NHS coupling Biop. Gel-NB (5-20 kDa) + 2-PEG-SH (3 4 kDa) NHS coupling Biop. Gel-NB (5-20 kDa) + 2-PEG-SH (3 4 kDa) NHS coupling Biop. Gel-NB (5-20 kDa) + 2-PEG-SH (3 4 kDa) NHS coupling Biop. Gel-NB (5-20 kDa) + 2-PEG-SH (3 4 kDa) NHS coupling Biop. Gel-NB (5-20 kDa) + 2-PEG-SH (3 4 kDa) NHS coupling Biop. Gel-NB (5-20 kDa) + 2-PEG-SH (3 4 kDa) NHS coupling Biop. Gel-NB (5-20 kDa) + 2-PEG-SH (3 4 kDa) NHS coupling Biop. Gel-NB (5-20 kDa) + 2-PEG-SH (3 4 kDa) NHS coupling Biop. Gel-NB (5-20 kDa) + 2-PEG-SH (3 4 kDa) NHS coupling Biop. Gel-NB (50 kDa) + 2-PEG-SH (3 4 kDa) NHS coupling Biop. Gel-NB (5-20 kDa) + 2-PEG-SH (3 4 kDa) NHS coupling Biop. Gel-NB (5-20 kDa) + 2-PEG-SH (3 4 kDa) NHS coupling Biop. Gel-NB (5-20 kDa) + 2-PEG-SH (3 4 kDa) NHS coupling Biop. Gel-NB (5-20 kDa) + 2-PEG-SH (5 4 kDa) NHS coupling Biop. Gel-NB (6.6	2.4			55
PEG 4-PEG-azide (10 kDa) + 8-PEG-allyne (20 kDa) Biop. HA-acryl. + di-SH PEG 4-PEG-vS (20 kDa) + di-SH PEG 4-PEG-vS (20 kDa) + di-SH A-PEG-vS (20 kDa) + di-SH 4-PEG-vS (20 kDa) + di-SH A-PEG-vS (20 kDa) + di-SH 4-PEG-vS (20 kDa) + di-SH A-PEG-vS (20 kDa) + di-SH 4-PEG-vS (20 kDa) + di-SH A-PEG-vS (20 kDa) + di-SH 4-PEG-vS (20 kDa) + di-SH A-PEG-vS (20 kDa) + di-SH 4-PEG-vS (20 kDa) + di-SH A-PEG-WAL (10 kDa) + 4-PEG-sH (10 kDa) 4-PEG-vS (20 kDa) + di-SH A-PEG-WAL (10 kDa) + 4-PEG-sH (10 kDa) 4-PEG-vS (20 kDa) + di-SH A-PEG-WAL (10 kDa) + 4-PEG-sH (10 kDa) 4-PEG-sH (10 kDa) A-PEG-WAL (10 kDa) + 4-PEG-sH (10 kDa) 4-PEG-sH (10 kDa) A-PEG-WAL (10 kDa) + 4-PEG-sH (10 kDa) 4-PEG-sH (10 kDa) A-PEG-WAL (10 kDa) + 4-PEG-sH (10 kDa) 4-PEG-sH (10 kDa) A-PEG-WAL (10 kDa) + 4-PEG-sH (10 kDa) 4-PEG-sH (10 kDa) A-PEG-WAL (10 kDa) + 4-PEG-sH (10 kDa) 4-PEG-sH (10 kDa) A-PEG-WAL (10 kDa) + 4-PEG-sH (10 kDa) 4-PEG-sH (10 kDa) A-ADA A-ADA (10 kDa) 4-PEG-sH (10 kDa) A-ADA A-ADA A-ADA A-ADA A-ADA		3.5		1.0		99
kDa)Enzym.Biop.kDa)Enzym.Biop.HA-acryl. + di:SHPEG4-PEG-VS (20 kDa) + di:SH4-PEG-VS (20 kDa) + di-SH4-PEG-VS (20 kDa)HA-NB + di-SH. Binder: 4-PEG-tetrazine(20 kDa)HA-NB + di-SH. Binder: 2-PEG-SH (3.4 kDa)NHS couplingBiop.Oc l-NB + 2-PEG-SH (3.4 kDa)NHS couplingBiop.RetrixBiop.Cel-NB + 2-PEG-SH (3.4 kDa)SupramolecularBiop.Cel-NB + 2-PEG-SH (3.4 kDa)AdmitrixBiop.Cel-NB + 2-PEG-SH (3.4 kDa)NHS couplingBiop.Cel-NB + 2-PEG-SH (3.4 kDa)NHS couplingBiop.Cel-NB + 2-PEG-SH (3.4 kDa)NHS couplingBiop.Cel-NB + 2-PEG-SH (10	I	2.1 - 3.3	I	78
Enzym.Biop.HA-acryl. + di:SHPEG+PEG-VS (20 kDa) + di:SHPEG+PEG-VS (20 kDa) + di:SH+PEG-VS (20 kDa) + di:SHHA-NB + di:SHHA-NB + di:SHBiop.HA-NB + di:SHBiop.HA-NB + di:SHBiop.HA-NB + di:SHBiop.Col kDa)HA-NB + di:SHBiop.Col kDa)HA-NB + di:SHBiop.HA-NB + di:SHBiop.Carboxy-cellul.AmtrixBiop.Carboxy-cellul.AmtrixBiop.Carboxy-cellul.AmontonPAMABiop.Carboxy-cellul.AmontonPAMAAmontonPAMABiop.Carboxy-cellul.AmontonPAMAAmontonPAMAAmontonPAMAAmontonPAMAAmontonPAMAAmontonPAMAAmontonPAMAAmontonPAMAAmontonPAMA						
tive Click Biop. HA-acryl. + di-SH PEG 4-PEG-VS (20 kDa) + di-SH 4-PEG-VS (20 kDa) + di-SH 4-PEG-tetrazine (20 kDa) 4-AMB + di-SH. Binder: 4-PEG-tetrazine (20 kDa) 4-ANB + di-SH. Binder: 4-PEG-tetrazine 4-ANB + di-SH. Binder: 2-PEG-SH (3,4 kDa) AANB + di-SH. Binder: 2-PEG-SH (3,4 kDa) AANB + di-SH AANB	74	3.5		0.9		99
PEG 4 -PEG-VS 20 (kDa) + di-SH 4 -PEG-VS 20 (kDa) 4 -ND 4 -SH. Binder: 4 -PEG-tetrazine 20 (kDa) 4 -SH. Binder: 2 -PEG-SH (3.4 kDa) 4 (kDa) 2 -PEG-NB (5-20 (kDa) + 22-PEG-SH (3.4 kDa) 4 (kDa) 2 -PEG-NB (5-20 (kDa) + 22-PEG-SH (3.4 kDa) 4 (kDa) 2 -PEG-NB (5-20 (kDa) + 22-PEG-SH (3.4 kDa) 4 (kDa) 2 -PEG-NB (5-20 (kDa) + 22-PEG-SH (3.4 kDa) 4 (kDa) 2 -PEG-NB (5-20 (kDa) + 22-PEG-SH (3.4 kDa) 4 (kDa)		3.5		1.5		68
4-PEG-VS 20 kDa) + di-SH 8-PEG-VS 20 kDa) + di-SH 4-PEG-VS 20 kDa) 4-AdNB + di-SH. Binder: 4-PEG-tetrazine (20 kDa) HA-NB + di-SH ander: di-SH (BA) NHS coupling Biop. (20 kDa) NHS NHS Cupla). Binder: 2-PEG-SH (3.4 kDa) NHS Biop. (20 kDa) NHS NHS Biop. (20 kDa) Matrix Biop.		5	0.3			67
8-PEG-VS (20 kDa) + di-SH 4-PEG-VS (20 kDa) + di-SH 4-PEG-VS (20 kDa) + di-SH 4-PEG-VS (20 kDa) + di-SH 4-PEG-MAL (10 kDa) + 4-PEG-FH (10 kDa) HAANB + di-SH. Binder: 4-PEG-fettrazine (20 kDa) HA-NB + di-SH. Binder: 4-PEG-SH (3.4 kDa) NHS coupling Biop. Gel-NB + 2-PEG-SH (3.4 kDa) Admer: 2-PEG-SH (3.4 kDa) NHS coupling Biop. Gel-NB + 2-PEG-SH (2 kDa). Binder: 4-PEG-SH (3.4 kDa) NHS coupling Biop.		4-12	0.5 - 2.6			70
tive Click Biop. 4-PEG-VS (20 kDa) + di-SH 4PEG-VS (20 kDa) + di-SH 4PEG-VS (20 kDa) + 4-PEG-KH (10 kDa) HA-AdNB + di-SH. Binder: HA-CD/AdNB HA-NB + di-SH. Binder: 4-PEG-tetrazine (20 kDa) HA-NB + di-SH. Binder: 4- KDa). Binder: 2-PEG-SH (3.4 kDa) NHS coupling Biop. Gel-NB + chito-MA Monom NHS coupling Sel-NB + chito-MA) + di-SH 100–107	3-12	0.5 - 13.5			71
tive Click Biop. HA-AdNB + di-SH Binder: HA-CD/AdNB HA-MCB + di-SH. Binder: HA-CD/AdNB HA-NB + di-SH. Binder: HA-CD/AdNB HA-NB + di-SH. Binder: 4-PEG-tetrazine (20 kDa) HA-NB + di-SH. Binder: 2-PEG-SH (3.4 kDa) Sunder: 2-PEG-SH (3.4 kDa) (20 kDa) HA-NB + di-SH. Binder: 2-PEG-SH (3.4 kDa) (20 kDa) HA-NB + di-SH. Binder: 2-PEG-SH (3.4 kDa) (20 kDa) HA-NB + di-SH. Binder: 2-PEG-SH (3.4 kDa) (20 kDa) HA-NB + di-SH. Binder: 2-PEG-SH (3.4 kDa) (20 kDa) HA-NB + di-SH. Binder: 2-PEG-SH (3.4 kDa) (20 kDa) HA-NB + di-SH. Binder: 2-PEG-SH (3.4 kDa) (20 kDa) HA-NB + di-SH. Binder: 2-PEG-SH (3.4 kDa) (20 kDa) HA-NB + di-SH. Binder: 2-PEG-SH (3.4 kDa) (20 kDa) HA-NB + di-SH (3.4 kDa) (20 kDa) HA-NB + di-SH (3.4 kDa) (20 kDa) HA-NB + di-SH (3.4 kDa) (20 kDa) (2		5	0.65			2
tive Click Biop. HAAdNB + di-SH. Binder: HA-CD/AdNB HA-NB + di-SH. Binder: HA-CD/AdNB HA-NB + di-SH. Binder: 4-PEG-tetrazine (20 kDa) HA-NB + di-SH. Binder: 4-PEG-sH (3.4 kDa). Binder: 2-PEG-SH (3.4 kDa) S-PEG-NB (5-20 kDa) + 2-PEG-SH (3.4 kDa). Binder: 2-PEG-SH (3.4 kDa) S-PEG-NB (5-20 kDa) + 2-PEG-SH (3.4 kDa). Binder: 2-PEG-SH (3.4 kDa) S-PEG-NB (5-20 kDa) + 2-PEG-SH (3.4 kDa) Matrix Biop. Gel-NB + 2-PEG-SH (3.4 kDa) Cel-NB + 2-PEG-SH (3.4 kDa) S-PEG-NB (5-20 kDa) + 2-PEG-SH (3.4 kDa) matrix Biop. Gel-NB + 2-PEG-SH (3.4 kDa) s-PEG-NB (5-20 kDa) + 2-PEG-SH (3.4 kDa) s-PEG-SH (2.0 kDa) + 2-PEG-SH (3.4 kDa) matrix Biop. Gel-NB + 2-PEG-SH (3.4 kDa) s-PEG-SH (2.0 kDa) + 2-PEG-SH (3.4 kDa) s-PEG-SH (2.0 kDa) + 2-PEG-SH (3.4 kDa) s-PEG-SH (3.4 kD		5	0.5			77
tive Click Biop. HAAdNB + di-SH. Binder: HA-CD/AdNB HA-NB + di-SH. Binder: 4-PEG-tetrazine (20 kDa) HA-NB + di-SH. Binder: 4-PEG-SH (3.4 kDa) S-PEG-NB (5-20 kDa) + 2-PEG-SH (3.4 kDa) (20 kDa). Binder:		1.8-2		9-18		75
HA-NB + di-SH. Binder: 4-PEG-tetrazine (20 kDa) HA-NB + di-SH. Binder: 4-PEG-SH (3.4 kDa) PEG 2-PEG-NB (5-20 kDa) + 2-PEG-SH (3.4 kDa) NHS coupling Biop. Cel-NB (5-20 kDa) + 2-PEG-SH (3.4 kDa) NHS coupling Biop. Gel-NB + 2-PEG-SH (2.4 kDa) Matrix Biop. Gel-NB + 2-PEG-SH (2.4 kDa) Matrix Biop. Gel-NB + 2-PEG-SH (3.4 kDa) Matrix Biop. Gel-NB + 2-PEG-SH (3.4 kDa) Matrix Biop. Gel-NB + 2-PEG-SH (3.4 kDa) Matrix Biop. Gel-NB + 2-PEG-SH (2.4 kDa) Matrix Biop. Gel-NB + 2-PEG-SH (2.4 kDa) Matrix Biop. Gel-NB + 2-PEG-SH (2.4 kDa) Matrix <td></td> <td>3</td> <td>9</td> <td> </td> <td> </td> <td>11</td>		3	9			11
(20 kDa) HA-NB + di-SH. Binder: 4-PEG-tetrazine (20 kDa) HA-NB + di-SH. Binder: 4-PEG-tetrazine (20 kDa) HA-NB + di-SH. Binder: 4-PEG-tetrazine (20 kDa) HA-NB + di-SH. Binder: 4-PEG-SH (3.4 kDa) S-PEG-NB (5-20 kDa) + 2-PEG-SH (3.4 kDa) CaP.NB (5-20 kDa) + 2-PEG-SH (3.4 kDa) S-PEG-NB (5-20 kDa) + 2-PEG-SH (3.4 kDa) NHS coupling Biop. Cel-NB + 2-PEG-SH (3.4 kDa) Cel-NB + 2-PEG-SH (3.4 kDa) CaP.NB (5-20 kDa) + 2-PEG-SH (3.4 kDa) NHS coupling Biop. Cel-NB + 2-PEG-SH (3.4 kDa) Cel-NB + 2-PEG-SH (3.4 kDa) CaP.NB (5-20 kDa) +		2.5	0.2			69
HA-NB + di-SH. Binder: 4-PEG-tetrazine (20 kDa) HA-NB + di-SH. Binder: 4-PEG-tetrazine (20 kDa) HA-NB + di-SH. Binder: 4-PEG-tetrazine (20 kDa) HA-NB + di-SH. Binder: 4-PEG-SH (3.4 kDa) S-PEG-NB (5-20 kDa) + 2-PEG-SH (3.4 kDa) Cal-NB (5-20 kDa) + 2-PEG-SH (3.4 kDa) S-PEG-NB (5-20 kDa) + 2-PEG-SH (3.4 kDa) S-PEG-SH (5.4 kDa) NHS coupling Biop. Cel-NB + 2-PEG-SH (3.4 kDa) Cel-NB + 2-PEG-SH (3.4 kDa) Cal-NB (5-20 kDa) + 2-PEG-SH (3.4 kDa) Biop. Cel-NB + 2-PEG-SH (3.4 kDa) Cel-NB + 2-PEG-SH (3.4 kDa) Cal-NB (5-20 kDa) + 2-PEG-SH (3.4 kDa) Cal-NB (5-20 kDa) + 2-PEG-SH (3.4 kDa) Biop. Cel-NB + 2-PEG-SH (3.4 kDa) Cel-NB + 2-PEG-SH (3.4 kDa) Cel-NB + 2-PEG-SH (3.4 kDa) Cal-NB (5-20 kDa) + 2-PEG-SH (5-						
 (20 kDa) HA-NB + di:SH. Binder: 4-PEG-tetrazine (20 kDa) HA-NB + di:SH. Binder: 4-PEG-tetrazine (20 kDa) HA-NB + di:SH. Binder: 4-PEG-tetrazine (20 kDa) Binder: 2-PEG-SH (3.4 kDa) 2-PEG-NB (5-20 kDa) + 2-PEG-SH (3.4 kDa) binder: 2-PEG-SH (3.4 kDa) 2-PEG-NB (5-20 kDa) NHS coupling Biop. Gel-NB + 2-PEG-SH (3.4 kDa) Binder: 2-PEG-SH (3.4 kDa) Biop. Gel-NB + 2-PEG-SH (3.4 kDa) Bioder: 2-PEG-SH (3.4 kDa) Bioder: 2-PEG-SH (3.4 kDa) A kDa). Binder: 4-kD3 A kDA-Sallol. Binder: 4-KD3 A kDA-Sallol. Binder: gallol + Ag⁺ A kDA-Sallol. Binder: gallol + Ag⁺ A kDA-SALLS AND MOND A kDA-SALLS AND MOND 		3.5	1.0		I	72
HA-NB + di-SH. Binder: 4-PEG-tetrazine (20 kDa) HA-NB + di-SH. Binder: di-SH (20 kDa) HA-NB + di-SH. Binder: di-SH PEG 2-PEG-NB (5-20 kDa) + 2-PEG-SH (3.4 kDa) NHS coupling Biop. RDa). Binder: 2-PEG-SH (3.4 kDa) NHS coupling Biop. RDa). Binder: 2-PEG-SH (3.4 kDa) NHS coupling Biop. Gel-NB + 2-PEG-SH (3.4 kDa) Matrix Biop. Gel-NB + 2-PEG-SH (2.4 kDa) Matrix Biop. Gel-NB + 4drito-MA Monon						
(20 kDa) HA-NB + di-SH. Binder: di-SH PEG 2-PEG-NB (5-20 kDa) + 2-PEG-SH (3.4 kDa) kDa). Binder: 2-PEG-SH (3.4 kDa) 2-PEG-NB (5-20 kDa) + 2-PEG-SH (3.4 kDa) NHS coupling Biop. 2-PEG-NB (5-20 kDa) + 2-PEG-SH (3.4 kDa) Matrix Biop. Gel-NB + 2-PEG-SH (2.4 kDa) Monom PMAS + chito-MA		9.7 - 15.0	0.3 - 2.0	1.6 - 4.5		73
PEG 2-PEG-NB (5-20 kDa) + 2-PEG-SH (3.4 kDa) PEG 2-PEG-NB (5-20 kDa) + 2-PEG-SH (3.4 kDa) RDa). Binder: 2-PEG-SH (3.4 kDa) 2-PEG-NB (5-20 kDa) + 2-PEG-SH (3.4 kDa) NHS coupling Biop. Cel-NB (20 kDa) 2-PEG-SH (3.4 kDa) Matrix Biop. Gel-NB (20 kDa) 2-PEG-SH (3.4 kDa) Matrix Biop. Gel-NB (20 kDa) Binder: 4-PEG-SH (3.4 kDa) Matrix Biop. Gel-NB (20 kDa) Binder: 4-PEG-SH (3.4 kDa) Matrix Biop. Gel-NB (20 kDa) Binder: 4-PEG-SH (3.4 kDa) Matrix Biop. Gel-NB (20 kDa) Binder: 4-PEG-SH (3.4 kDa) PEG-NHS (20 kDa) Binder: 9-FEG-SH (3.4 kDa) n chemistry Supramolecular Biop. Gel-NA - Gallot. Binder: gel-NG Admonter gallot + Ag ⁺ eractions Supramolecular Biop. Gel-MA + chito-MA Monon PMAS						
PEG 2-PEG-NB (5-20 kDa) + 2-PEG-SH (3.4 kDa) kDa). Binder: 2-PEG-SH (3.4 kDa) 2-PEG-NB (5-20 kDa) + 2-PEG-SH (3.4 kDa) RDa). Binder: 2-PEG-SH (2.4 kDa) RDA RDA <t< td=""><td></td><td>2</td><td> </td><td>л С</td><td> </td><td>43</td></t<>		2		л С		43
kDa). Binder: 2-PEG-SH (3.4 kDa) 2-PEG-NB (5-20 kDa) + 2-PEG-SH (3.4 kDa) NHS coupling Biop. RDa). Binder: 2-PEG-SH (3.4 kDa) NHS coupling Biop. Gel-NB (5-20 kDa) + 2-PEG-SH (3.4 kDa) Matrix Biop. Gel-NB (20 kDa) Matrix Biop. Gel-NB (20 kDa) Matrix Biop. Gel-TG. Binder: gel-TG n chemistry Supramolecular Biop. Gel-TG. Binder: gel-TG eractions Supramolecular Biop. Gel-MA + chito-MA Monom PMSS + MPTC		11.3 - 15.1	0.2 - 1.5			44
2-PEG-NB (5-20 kDa) + 2-PEG-SH (3.4 kDa). Binder: 2-PEG-SH (3.4 kDa) NHS coupling Biop. Gel-NB + 2-PEG-SH (2 kDa). Binder: 4- PEG-NHS (20 kDa) Matrix Biop. Gel-TG. Binder: gel-TG Gel-TG. Binder: gel-TG Antrix Supramolecular Biop. Gel-MS (20 kDa) HA-MA-gallol. Binder: 4- hA-MA-gallol. Binder: gallol + Ag ⁺ eractions Supramolecular Biop. Gel-MA + chito-MA	2G-SH (3.4 kDa)					
kDa), Binder: 2-PEG-SH (3.4 kDa) NHS coupling Biop. Gel-NB + 2-PEG-SH (2 kDa), Binder: 4- PEG-NHS (20 kDa) Matrix Biop. Gel-TG. Binder: gel-TG Gel-TG. Binder: gel-TG HA-MA-gallol. Binder: gallol + Ag ⁺ eractions Supramolecular Biop. Gel-MA + chito-MA Monom PnaSS + MPTC	Da) + 2-PEG-SH (3.4 200–500	10 - 15	1			76
NHS coupling Biop. Gel-NB + 2-PEG-SH (2 kDa). Binder: 4- ReG-NHS (20 kDa) Matrix Biop. Gel-TG. Binder: gel-TG n chemistry Supramolecular Biop. Gel-TG. Binder: gel-TG n chemistry Supramolecular Biop. Gel-TG. Binder: gel-TG eractions Supramolecular Biop. Carboxy-cellul. nanofibrils eractions Supramolecular Biop. Gel-MA + chito-MA Monom PMSS_MA PMSS_MA PMSS_MA	CG-SH (3.4 kDa)					
PEG-NHS (20 kDa) Matrix Biop. Gel-TG. Binder: gel-TG on chemistry Supramolecular Biop. Carboxy-cellul. nanofibrils HA-MA-gallol. Binder: gallol + Ag ⁺ eractions Supramolecular Biop. Gel-MA + chito-MA Monom PnaSS + MPTC		4	2	1.5		82
Matrix Biop. Gel-TG. Binder: gel-TG on chemistry Supramolecular Biop. Carboxy-cellul. nanofibrils HA-MA-gallol. Binder: gallol + Ag ⁺ eractions Supramolecular Biop. Gel-MA + chito-MA Monom PnaSS + MPTC						
in chemistry Supramolecular Biop. Carboxy-cellul. nanofibrils HA-MA-gallol. Binder: gallol + Ag ⁺ eractions Supramolecular Biop. Gel-MA + chito-MA Monom PnaSS + MPTC	el-TG 120–300	5-15			14.4 - 56.8	83
HA-MA-gallol. Binder: gallol + Ag ⁺ eractions Supramolecular Biop. Gel-MA + chito-MA Monom PnaSS + MPTC		1	0.7 - 1.0			84
eractions Supramolecular Biop. Gel-MA + chito-MA Monom PnaSS + MPTC	der: gallol + Ag ⁺ —	I	0.13			13
Monom PnaSS + MPTC		10	3.1			52
	I	58			4000	51
IIIUCI. IIEUW. DOUDIC. IIEUW. MOUOIII. FAMPS + FAM 10-200	10-200			Ι	250	10
PAMPS + PAM 65	65	13.6 - 45.7			20 - 570	14

Review

far beyond tissue engineering, for example as synthetic loadbearing materials (Table 1).

4. Conclusion

Granular hydrogels are a promising class of materials, for their ease of processing, the possibility to abruptly change their composition, and the ability to tune their mechanical properties over a wide range. These assets render granular hydrogels especially attractive for applications in bioengineering and soft robotics. The size of microgels, and hence the microstructure of granular hydrogels, can be closely controlled with the size of the emulsion drops they are made from. The composition and mechanical properties of microgels can be closely controlled by taking advantage of the vast knowhow on the compositionstructure-mechanical property relationship of bulk hydrogels. However, the potential of granular hydrogels has not been fully exploited yet because little attention has been given to the interparticle linking strategy that is decisive in the mechanical properties of granular hydrogels. As a result, currently employed granular hydrogels are mechanically weak such that they are primarily used for tissue engineering. To extend the field of use of granular hydrogels to load-bearing applications, a better understanding of the influence of inter-particle interactions on the mechanical properties of granular hydrogels is key. This advanced understanding would allow the fabrication of injectable and 3D printable hydrogels with tuneable load-bearing mechanical properties that have the potential to strongly advance fields where hydrogels are rarely used today including soft robotics and tissue replacements.

5. Future perspective

Despite the growing interest in granular hydrogels, a detailed understanding of the influence of microstructure and local composition on their mechanical properties, including stiffness and toughness remains to be established. For example, in many systems, it is not clear how load is transferred between the different microparticles, and hence, how stress is distributed within them. This question becomes especially pertinent in systems that are composed of highly jammed microgels: highly jammed microgels tend to trap air that forms voids. These voids present defects within granular hydrogels that most likely cause stress concentrations, thereby significantly reducing their stretchability. However, systematic studies on the effect of voids on the stretchability of granular hydrogels and how such voids can be avoided remain to be done. A better understanding when and where stress concentrations occur would likely enable the design of granular hydrogels that are much tougher than the currently available counterparts as stress could be distributed over much larger areas. We demonstrated the potential of this strategy on double network granular hydrogels that displayed a 4-fold higher stiffness than any of the previously reported 3D printed hydrogels. This enhanced stiffness can be assigned to a more efficient load transfer across microgels that avoids stress concentrations at the interparticle interface.

Microgels are often synthesized from soft hydrogels. Upon jamming, these microgels deform to increase their packing fraction. While the packing of hard spheres has been studied in detail, much less is known on the packing of soft deformable counterparts. For example, it is still unclear how the size and polydispersity of soft microgels influence their packing and propensity to form air inclusions that serve as defects. Importantly, the deformation of microgels is accompanied with an increase in their contact area. This increased contact area offers new possibilities to increase the density of surface localized inter-microgel connections, and hence, the efficiency to transfer load between adjacent microgels. However, the influence of the stiffness of microgels on their degree of deformation upon jamming and hence, the intermicrogel contact area remains to be determined. As a result, very little is known on the influence of the density of surfacelocalized inter-microgel connections on the overall stiffness and toughness of the resulting granular hydrogels. Understanding this parameter would enable the engineering of granular hydrogels possessing a reduced brittleness and expanding their application potential as engineered soft materials.

A key advantage of granular hydrogels is the possibility to abruptly change their composition by forming them from microgels possessing different compositions. This possibility bears enormous potential as it allows introducing different functionalities into these materials. However, up to now, this potential has not been fully explored. As a result, we do not know how local composition of these materials influence their mechanical properties and response to external stimuli. We expect fundamental research on the influence of structure and local composition of granular hydrogels on their mechanical properties and functionality to enable their widespread adoption as load-bearing support matrix for tissue engineering, and to open up new fields of their use, for example, as load-bearing soft hydrated actuators and sensors in soft robotics.

Author contributions

All authors contributed to the writing of the review and edited it.

Conflicts of interest

There are no conflicts to declare.

Notes and references

- 1 H. Yuk, *et al.* Dry double-sided tape for adhesion of wet tissues and devices, *Nature*, 2019, **575**, 169–174.
- 2 J. Fang, *et al.* Injectable Drug-Releasing Microporous Annealed Particle Scaffolds for Treating Myocardial Infarction, *Adv. Funct. Mater.*, 2020, **30**, 2004307.
- 3 J. A. Brassard, M. Nikolaev, T. Hübscher, M. Hofer and M. P. Lutolf, Recapitulating macro-scale tissue self-organization through organoid bioprinting, *Nat. Mater.*, 2021, **20**, 22–29.
- 4 B. V. Slaughter, S. S. Khurshid, O. Z. Fisher, A. Khademhosseini and N. A. Peppas, Hydrogels in Regenerative Medicine, *Adv. Mater.*, 2009, **21**, 3307–3329.

- 5 Y. Sun, *et al.* 3D bioprinting dual-factor releasing and gradient-structured constructs ready to implant for anisotropic cartilage regeneration, *Sci. Adv.*, 2020, **6**, eaay1422.
- 6 A. C. Daly, L. Riley, T. Segura and J. A. Burdick, Hydrogel microparticles for biomedical applications, *Nat. Rev. Mater.*, 2020, 5, 20–43.
- 7 L. Riley, L. Schirmer and T. Segura, Granular hydrogels: emergent properties of jammed hydrogel microparticles and their applications in tissue repair and regeneration, *Curr. Opin. Biotechnol.*, 2019, **60**, 1–8.
- 8 H. Du, A. Cont, M. Steinacher and E. Amstad, Fabrication of Hexagonal-Prismatic Granular Hydrogel Sheets, *Langmuir*, 2018, 34, 3459–3466.
- 9 N. J. Darling, E. Sideris, N. Hamada, S. T. Carmichael and T. Segura, Injectable and Spatially Patterned Microporous Annealed Particle (MAP) Hydrogels for Tissue Repair Applications, *Adv. Sci.*, 2018, **5**, 1801046.
- 10 R. Takahashi, *et al.* Tough Particle-Based Double Network Hydrogels for Functional Solid Surface Coatings, *Adv. Mater. Interfaces*, 2018, **5**, 1801018.
- 11 J. E. Mealy, *et al.* Injectable Granular Hydrogels with Multifunctional Properties for Biomedical Applications, *Adv. Mater.*, 2018, **30**, 1705912.
- 12 M. H. Chen, *et al.* Injectable Supramolecular Hydrogel/ Microgel Composites for Therapeutic Delivery, *Macromol. Biosci.*, 2019, **19**, 1800248.
- 13 M. Shin, K. H. Song, J. C. Burrell, D. K. Cullen and J. A. Burdick, Injectable and Conductive Granular Hydrogels for 3D Printing and Electroactive Tissue Support, *Adv. Sci.*, 2019, 6, 1901229.
- 14 M. Hirsch, A. Charlet and E. Amstad, 3D Printing of Strong and Tough Double Network Granular Hydrogels, *Adv. Funct. Mater.*, 2021, **31**, 2005929.
- 15 E. A. Guzzi and M. W. Tibbitt, Additive Manufacturing of Precision Biomaterials, *Adv. Mater.*, 2020, **32**, 1901994.
- 16 W. Sun, *et al.* The bioprinting roadmap, *Biofabrication*, 2020, 12, 022002.
- 17 T. H. Qazi and J. A. Burdick, Granular hydrogels for endogenous tissue repair, *Biomaterials and Biosystems*, 2021, 1, 100008.
- 18 S. R. Caliari and J. A. A. Burdick, Practical Guide to Hydrogels for Cell Culture, *Nat. Methods*, 2016, 13, 405–414.
- 19 J. C. Rose and L. D. Laporte, Hierarchical Design of Tissue Regenerative Constructs, *Adv. Healthcare Mater.*, 2018, 7, 1701067.
- 20 D. Zhu, P. Trinh, E. Liu and F. Yang, Biochemical and Mechanical Gradients Synergize To Enhance Cartilage Zonal Organization in 3D, *ACS Biomater. Sci. Eng.*, 2018, 4, 3561–3569.
- 21 J. R. Tse and A. J. Engler, Stiffness Gradients Mimicking In Vivo Tissue Variation Regulate Mesenchymal Stem Cell Fate, PLoS One, 2011, 6, e15978.
- 22 O. Chaudhuri, Viscoelastic hydrogels for 3D cell culture, *Biomater. Sci.*, 2017, **5**, 1480–1490.

- 23 J. L. Balestrini, S. Chaudhry, V. Sarrazy, A. Koehler and B. Hinz, The mechanical memory of lung myofibroblasts, *Integr. Biol.*, 2012, **4**, 410–421.
- 24 O. Chaudhuri, *et al.* Hydrogels with tunable stress relaxation regulate stem cell fate and activity, *Nat. Mater.*, 2016, **15**, 326–334.
- 25 M. Nikolaev, *et al.* Homeostatic mini-intestines through scaffold-guided organoid morphogenesis, *Nature*, 2020, **585**, 574–578.
- 26 M. Shur, *et al.* Soft Printable Electrode Coating for Neural Interfaces, *ACS Appl. Bio Mater.*, 2020, **3**, 4388–4397.
- 27 J. Yang, Y. S. Zhang, K. Yue and A. Khademhosseini, Cellladen hydrogels for osteochondral and cartilage tissue engineering, *Acta Biomater.*, 2017, 57, 1–25.
- 28 X. Zhao, *et al.* Soft Materials by Design: Unconventional Polymer Networks Give Extreme Properties, *Chem. Rev.*, 2021, **121**, 4309–4372.
- 29 Y. J. No, *et al.* High-Strength Fiber-Reinforced Composite Hydrogel Scaffolds as Biosynthetic Tendon Graft Material, *ACS Biomater. Sci. Eng.*, 2020, **6**, 1887–1898.
- 30 G. Yang, H. Lin, B. B. Rothrauff, S. Yu and R. S. Tuan, Multilayered polycaprolactone/gelatin fiber-hydrogel composite for tendon tissue engineering, *Acta Biomater.*, 2016, 35, 68–76.
- 31 P. Karami, *et al.* Composite Double-Network Hydrogels To Improve Adhesion on Biological Surfaces, *ACS Appl. Mater. Interfaces*, 2018, **10**, 38692–38699.
- 32 J. P. Gong, Y. Katsuyama, T. Kurokawa and Y. Osada, Double-Network Hydrogels with Extremely High Mechanical Strength, *Adv. Mater.*, 2003, **15**, 1155–1158.
- 33 J.-Y. Sun, et al. Highly stretchable and tough hydrogels, Nature, 2012, 489, 133–136.
- 34 J. Kim, G. Zhang, M. Shi and Z. Suo, Fracture, fatigue, and friction of polymers in which entanglements greatly outnumber cross-links, *Science*, 2021, **374**, 212–216.
- 35 S. M. Naqvi, *et al.* Living Cell Factories Electrosprayed Microcapsules and Microcarriers for Minimally Invasive Delivery, *Adv. Mater.*, 2016, **28**, 5662–5671.
- 36 V. G. Muir, T. H. Qazi, J. Shan, J. Groll and J. A. Burdick, Influence of Microgel Fabrication Technique on Granular Hydrogel Properties, *ACS Biomater. Sci. Eng.*, 2021, 7, 4269– 4281.
- 37 J. W. Nichol, *et al.* Cell-laden microengineered gelatin methacrylate hydrogels, *Biomaterials*, 2010, **31**, 5536–5544.
- 38 D. Dendukuri, D. C. Pregibon, J. Collins, T. A. Hatton and P. S. Doyle, Continuous-flow lithography for highthroughput microparticle synthesis, *Nat. Mater.*, 2006, 5, 365–369.
- 39 H. Yuk, *et al.* Rapid and coagulation-independent haemostatic sealing by a paste inspired by barnacle glue, *Nat. Biomed. Eng.*, 2021, **5**, 1131–1142.
- 40 P.-H. Kim, *et al.* Injectable multifunctional microgel encapsulating outgrowth endothelial cells and growth factors for enhanced neovascularization, *J. Controlled Release*, 2014, **187**, 1–13.

- 41 A. Sheikhi, *et al.* Microfluidic-enabled bottom-up hydrogels from annealable naturally-derived protein microbeads, *Biomaterials*, 2019, **192**, 560–568.
- 42 B. Cai, *et al.* Injectable Gel Constructs with Regenerative and Anti-Infective Dual Effects Based on Assembled Chitosan Microspheres, *ACS Appl. Mater. Interfaces*, 2018, **10**, 25099– 25112.
- 43 C. B. Highley, K. H. Song, A. C. Daly and J. A. Burdick, Jammed Microgel Inks for 3D Printing Applications, *Adv. Sci.*, 2019, **6**, 1801076.
- 44 S. Xin, O. M. Wyman and D. L. Alge, Assembly of PEG Microgels into Porous Cell-Instructive 3D Scaffolds *via* Thiol–Ene Click Chemistry, *Adv. Healthcare Mater.*, 2018, 7, 1800160.
- 45 E. Weeks, Soft jammed materials, in *Statistical Physics of Complex Fluids*, Tohoku University Press, 2007, vol. 2, pp. 1–87.
- 46 A. J. Liu and S. R. Nagel, Jamming is not just cool any more, *Nature*, 1998, **396**, 21–22.
- 47 P. Menut, S. Seiffert, J. Sprakel and D. A. Weitz, Does size matter? Elasticity of compressed suspensions of colloidaland granular-scale microgels, *Soft Matter*, 2011, 8, 156–164.
- 48 D. J. Hornbaker, R. Albert, I. Albert, A.-L. Barabási and P. Schiffer, What keeps sandcastles standing?, *Nature*, 1997, **387**, 765.
- 49 T. J. Hinton, *et al.* Three-dimensional printing of complex biological structures by freeform reversible embedding of suspended hydrogels, *Sci. Adv.*, 2015, **1**, e1500758.
- 50 C. Pellet and M. Cloitre, The glass and jamming transitions of soft polyelectrolyte microgel suspensions, *Soft Matter*, 2016, **12**, 3710–3720.
- 51 F. Luo, *et al.* Oppositely Charged Polyelectrolytes Form Tough, Self-Healing, and Rebuildable Hydrogels, *Adv. Mater.*, 2015, 27, 2722–2727.
- 52 R.-S. Hsu, *et al.* Adaptable Microporous Hydrogels of Propagating NGF-Gradient by Injectable Building Blocks for Accelerated Axonal Outgrowth, *Adv. Sci.*, 2019, **6**, 1900520.
- 53 T. Y. Lee, C. A. Guymon, E. S. Jönsson and C. E. Hoyle, The effect of monomer structure on oxygen inhibition of (meth)acrylates photopolymerization, *Polymer*, 2004, **45**, 6155–6162.
- 54 O. Jeon, Y. B. Lee, T. J. Hinton, A. W. Feinberg and E. Alsberg, Cryopreserved cell-laden alginate microgel bioink for 3D bioprinting of living tissues, *Mater. Today Chem.*, 2019, **12**, 61–70.
- 55 B. N. Pfaff, et al. Selective and Improved Photoannealing of Microporous Annealed Particle (MAP) Scaffolds, ACS Biomater. Sci. Eng., 2021, 7, 422–427.
- 56 N. Zoratto, *et al. In situ* forming microporous gelatin methacryloyl hydrogel scaffolds from thermostable microgels for tissue engineering, *Bioeng. Transl. Med.*, 2020, 5, e10180.
- 57 M. Choppadandi, N. More and G. Kapusetti, Detoxification of poly(methyl methacrylate) bone cement by natural antioxidant intervention, *J. Biomed. Mater. Res., Part A*, 2019, **107**, 2835–2847.

- 58 H. C. Kolb, M. G. Finn and K. B. Sharpless, Click Chemistry: Diverse Chemical Function from a Few Good Reactions, *Angew. Chem., Int. Ed.*, 2001, 40, 2004–2021.
- 59 F. Jivan, *et al.* Sequential Thiol–Ene and Tetrazine Click Reactions for the Polymerization and Functionalization of Hydrogel Microparticles, *Biomacromolecules*, 2016, 17, 3516–3523.
- 60 T. E. Brown and K. S. Anseth, Spatiotemporal hydrogel biomaterials for regenerative medicine, *Chem. Soc. Rev.*, 2017, **46**, 6532–6552.
- 61 M. P. Lutolf, N. Tirelli, S. Cerritelli, L. Cavalli and J. A. Hubbell, Systematic Modulation of Michael-Type Reactivity of Thiols through the Use of Charged Amino Acids, *Bioconjugate Chem.*, 2001, **12**, 1051–1056.
- 62 M. P. Lutolf and J. A. Hubbell, Synthesis and Physicochemical Characterization of End-Linked Poly(ethylene glycol)-*co*-peptide Hydrogels Formed by Michael-Type Addition, *Biomacromolecules*, 2003, 4, 713–722.
- 63 D. P. Nair, *et al.* The Thiol-Michael Addition Click Reaction: A Powerful and Widely Used Tool in Materials Chemistry, *Chem. Mater.*, 2014, 26, 724–744.
- 64 R. Cruz-Acuña, *et al.* Synthetic hydrogels for human intestinal organoid generation and colonic wound repair, *Nat. Cell Biol.*, 2017, **19**, 1326–1335.
- 65 E. A. Phelps, *et al.* Maleimide cross-linked bioactive PEG hydrogel exhibits improved reaction kinetics and cross-linking for cell encapsulation and *in situ* delivery, *Adv. Mater.*, 2012, **24**, 64–70.
- 66 E. Sideris, *et al.* Particle Hydrogels Based on Hyaluronic Acid Building Blocks, *ACS Biomater. Sci. Eng.*, 2016, **2**, 2034–2041.
- 67 D. R. Griffin, W. M. Weaver, P. O. Scumpia, D. Di Carlo and T. Segura, Accelerated wound healing by injectable microporous gel scaffolds assembled from annealed building blocks, *Nat. Mater.*, 2015, **14**, 737–744.
- 68 L. R. Nih, E. Sideris, S. T. Carmichael and T. Segura, Injection of Microporous Annealing Particle (MAP) Hydrogels in the Stroke Cavity Reduces Gliosis and Inflammation and Promotes NPC Migration to the Lesion, *Adv. Mater.*, 2017, **29**, 1606471.
- 69 N. F. Truong, S. C. Lesher-Pérez, E. Kurt and T. Segura, Pathways Governing Polyethylenimine Polyplex Transfection in Microporous Annealed Particle Scaffolds, *Bioconjugate Chem.*, 2019, 30, 476–486.
- 70 J. Koh, *et al.* Enhanced *In Vivo* Delivery of Stem Cells using Microporous Annealed Particle Scaffolds, *Small*, 2019, 15, 1903147.
- 71 J. M. de Rutte, J. Koh and D. D. Carlo, Scalable High-Throughput Production of Modular Microgels for *In Situ* Assembly of Microporous Tissue Scaffolds, *Adv. Funct. Mater.*, 2019, **29**, 1900071.
- 72 N. F. Truong, *et al.* Microporous annealed particle hydrogel stiffness, void space size, and adhesion properties impact cell proliferation, cell spreading, and gene transfer, *Acta Biomater.*, 2019, **94**, 160–172.
- 73 N. J. Darling, *et al.* Click by Click Microporous Annealed Particle (MAP) Scaffolds, *Adv. Healthcare Mater.*, 2020, **9**, 1901391.

- 74 L. J. Pruett, C. H. Jenkins, N. S. Singh, K. J. Catallo and D. R. Griffin, Heparin Microislands in Microporous Annealed Particle Scaffolds for Accelerated Diabetic Wound Healing, *Adv. Funct. Mater.*, 2021, **31**, 2104337.
- 75 L. Pruett, *et al.* Development of a microporous annealed particle hydrogel for long-term vocal fold augmentation, *Laryngoscope*, 2020, **130**, 2432–2441.
- 76 S. Xin, D. Chimene, J. E. Garza, A. K. Gaharwar and D. L. Alge, Clickable PEG hydrogel microspheres as building blocks for 3D bioprinting, *Biomater. Sci.*, 2019, 7, 1179–1187.
- 77 D. R. Griffin, *et al.* Activating an adaptive immune response from a hydrogel scaffold imparts regenerative wound healing, *Nat. Mater.*, 2021, **20**, 560–569.
- 78 A. S. Caldwell, G. T. Campbell, K. M. T. Shekiro and K. S. Anseth, Clickable Microgel Scaffolds as Platforms for 3D Cell Encapsulation, *Adv. Healthcare Mater.*, 2017, 6, 1700254.
- 79 N. A. Kurniawan, *et al.* Buffers Strongly Modulate Fibrin Self-Assembly into Fibrous Networks, *Langmuir*, 2017, **33**, 6342–6352.
- 80 R. Eelkema and A. Pich, Pros and Cons: Supramolecular or Macromolecular: What Is Best for Functional Hydrogels with Advanced Properties?, *Adv. Mater.*, 2020, **32**, 1906012.
- 81 N. Rauner, M. Meuris, M. Zoric and J. C. Tiller, Enzymatic mineralization generates ultrastiff and tough hydrogels with tunable mechanics, *Nature*, 2017, **543**, 407–410.

- 82 F. Li, *et al.* Cartilage tissue formation through assembly of microgels containing mesenchymal stem cells, *Acta Biomater.*, 2018, 77, 48–62.
- 83 K. Song, A. M. Compaan, W. Chai and Y. Huang, Injectable Gelatin Microgel-Based Composite Ink for 3D Bioprinting in Air, *ACS Appl. Mater. Interfaces*, 2020, **12**, 22453–22466.
- 84 D. B. Gehlen, et al. Granular Cellulose Nanofibril Hydrogel Scaffolds for 3D Cell Cultivation, Macromol. Rapid Commun., 2020, 41, 2000191.
- 85 H. Lee, N. F. Scherer and P. B. Messersmith, Single-molecule mechanics of mussel adhesion, *Proc. Natl. Acad. Sci. U. S. A.*, 2006, **103**, 12999–13003.
- 86 E. Khare, N. Holten-Andersen and M. J. Buehler, Transitionmetal coordinate bonds for bioinspired macromolecules with tunable mechanical properties, *Nat. Rev. Mater.*, 2021, 6, 421–436.
- 87 A. Charlet, V. Lutz-Bueno, R. Mezzenga and E. Amstad, Shape retaining self-healing metal-coordinated hydrogels, *Nanoscale*, 2021, **13**, 4073–4084.
- 88 J. Hu, *et al.* Microgel-Reinforced Hydrogel Films with High Mechanical Strength and Their Visible Mesoscale Fracture Structure, *Macromolecules*, 2011, 44, 7775–7781.
- 89 A. Charlet, M. Hirsch, S. Schreiber and E. Amstad, Recycling of Load-Bearing 3D Printable Double Network Granular Hydrogels, *Small*, 2022, 2107128.